

## Article

# Effect of Polypyrrole-Fe<sub>3</sub>O<sub>4</sub> Composite Modified Anode and Its Electrodeposition Time on the Performance of Microbial Fuel Cells

Liping Fan <sup>1,2,\*</sup> and Yaobin Xi <sup>2</sup><sup>1</sup> College of Information Engineering, Shenyang University of Chemical Technology, Shenyang 110142, China<sup>2</sup> College of Environment and Safety Engineering, Shenyang University of Chemical Technology, Shenyang 110142, China; xiyaobin1@163.com

\* Correspondence: fanliping@syuct.edu.cn

**Abstract:** Anode modification is a useful method to increase the performance of microbial fuel cells (MFCs). By using the electrochemical deposition method, Fe<sub>3</sub>O<sub>4</sub> and polypyrrole (PPy) were polymerized on a carbon felt anode to prepare Fe<sub>3</sub>O<sub>4</sub>-PPy composite modified anodes. In order to ascertain the effect of electrodeposition time on characteristics of the modified electrode, the preparation time of the modified electrode was adjusted. The modified anodes were used in MFCs, and their performances were evaluated by analyzing the electricity generation performance and sewage treatment capacity of MFCs. Experimental results indicated that the Fe<sub>3</sub>O<sub>4</sub>-PPy composite modified anodes could enhance the power production capacity and sewage treatment efficiency of MFC effectively. In particular, when the deposition time was 50 min, the modified anode could significantly improve the MFC performance. In this case, the steady-state current density of MFC increased by 59.5% in comparison with that of the MFC with an unmodified carbon felt anode, and the chemical oxygen demand (COD) removal rate was 95.3% higher than that of the unmodified anode. Therefore, the Fe<sub>3</sub>O<sub>4</sub>-PPy composite is an effective material for electrode modification, and a good anode modification effect can be obtained by selecting the appropriate electrodeposition time.

**Keywords:** microbial fuel cell; anode modification; polypyrrole; Fe<sub>3</sub>O<sub>4</sub>



**Citation:** Fan, L.; Xi, Y. Effect of Polypyrrole-Fe<sub>3</sub>O<sub>4</sub> Composite Modified Anode and Its Electrodeposition Time on the Performance of Microbial Fuel Cells. *Energies* **2021**, *14*, 2461. <https://doi.org/10.3390/en14092461>

Academic Editor: Antonino S. Arico

Received: 9 March 2021

Accepted: 23 April 2021

Published: 26 April 2021

**Publisher's Note:** MDPI stays neutral with regard to jurisdictional claims in published maps and institutional affiliations.



**Copyright:** © 2021 by the authors. Licensee MDPI, Basel, Switzerland. This article is an open access article distributed under the terms and conditions of the Creative Commons Attribution (CC BY) license (<https://creativecommons.org/licenses/by/4.0/>).

## 1. Introduction

Up to now, fossil fuels remain the main energy source for our daily life and industrial and agricultural production. Excessive exploitation and use of fossil fuels not only causes resource exhaustion, but also causes serious environmental pollution [1–3]. Nowadays, the two problems of lack of energy source and pollution of environment have become bottleneck problems that restrict the sustainable development of human society and even threaten the survival of human beings and the fate of the Earth. Developing renewable energy systems that can replace fossil fuels has become a key issue to be solved urgently [4–6].

Due to the potential functionality in wastewater treatment and bioenergy production, MFC is regarded as a promising green power generation technology and a new sewage treatment process with many benefits such as cleanliness, effectiveness, recyclability, and less toxic products [7–10]. However, MFC has low power output in the current research, which restricts its practical application [11].

The performance of MFC is affected by many factors. For example, electrode, electrode spacing, microbial population, proton exchange membrane, internal and external resistance, etc. will have an impact on the performance of MFCs [12–14]. As an important part of microbial growth and electron collection, the physical, chemical properties, and surface characteristics of the anode directly affect the attachment growth and electron transfer ability of exoelectrogens on its surface, thus greatly affecting the power production capacity and sewage disposal effect of microbial fuel cell [15–18]. High performance anode materials

for MFC should have the characteristics of high conductivity, large specific surface area, biocompatibility, low cost, and corrosion resistance [19]. Carbon-based materials are the most widely used anode materials in MFCs due to their low cost, strong biocompatibility, high conductivity, and good chemical stability [20,21]. However, due to the finite specific surface area, poor bacterial adhesion, low toughness, and little electrocatalytic activity of carbon-based anode, it is difficult for MFC to achieve ideal performance [22,23].

The modification of anode materials can improve the performance of MFCs [24,25]. On the basis of traditional carbon-based materials, researchers had found that metal oxides [26,27], carbon nanotubes [28,29], conductive polymers [30–32], and graphene [33,34] can be used for anode modification. Metal materials are widely used in the electrochemical field because of their high conductivity and high catalytic activity. However, the cost of metals with better conductivity is relatively high, and it is difficult to promote large-scale use. The catalytic activity of non-noble metals and their oxide nanoparticles are basically equivalent to that of precious metals; in addition, they can greatly reduce the resistance during operation and increase the adhesion of microorganisms on the electrode [35]; also, they can save costs and thus are very promising anode modification materials.  $\text{Fe}_3\text{O}_4$  is widely used as an anode modifier as a conductive metal oxide among non-noble metals, which is mainly to improve the kinetic activity of the anode reaction. The power generation of MFC with the  $\text{Fe}_3\text{O}_4$  modified anode is higher than that without modification, which indicates that the  $\text{Fe}_3\text{O}_4$  modified anode can effectively increase the performance of MFC [36].

Conductive polymers are used as common materials for MFC anode modification due to their excellent biocompatibility [37]. Among them, polypyrrole (PPy) is widely used in the modification of anodes and supercapacitors due to its high charge storage capacity [38,39]. The results of the PPy modified graphite felt anode showed that biofilm was formed on the modified anode, which improved the surface roughness of the anode and provided favorable conditions for microorganisms to attach, thus greatly improving the conductivity of the anode after and enhancing the power density [40].

Our research attempts to raise the generating capacity and sewage disposal effect of MFCs by finding some simple, low-cost, and efficient anode modification methods. In this article, the effects of a polypyrrole- $\text{Fe}_3\text{O}_4$  composite modified anode and its electrodeposition time on the performance of MFCs were investigated experimentally. The synergistic effect of conductive polymers and metal oxides was introduced to ameliorate the properties of the anode. The  $\text{Fe}_3\text{O}_4$ -PPy<sub>10</sub>/CF (carbon felt),  $\text{Fe}_3\text{O}_4$ -PPy<sub>30</sub>/CF,  $\text{Fe}_3\text{O}_4$ -PPy<sub>50</sub>/CF, and  $\text{Fe}_3\text{O}_4$ -PPy<sub>70</sub>/CF composite modified electrodes were prepared by controlling the deposition time, the effect of carbon felt anodes polymerized with PPy at different times on the power generating capacity, and the sewage disposal effect of MFC was tested and analyzed, and thus the best electrodeposition time for anodic modification with the  $\text{Fe}_3\text{O}_4$ -PPy composite material was determined.

## 2. Materials and Methods

### 2.1. Structure of the Experimental System

The experimental system was made up of the following instruments and equipment: a dual-chamber MFC, an external load, and a data acquisition system (Figure 1). The dual-chamber MFC was composed of an anode chamber and a cathode chamber separated by a proton exchange membrane in the middle, and electrodes were placed in the chamber. The anode chamber and the cathode chamber were made of two organic glass chambers with a volume of 500 mL. The electrode materials were carbon felt with the size of 4 cm × 5 cm × 0.5 cm. The real-time output voltage produced by MFC was gathered by a data acquisition card (MPS-010602; Beijing Morpheus Electronic Technology Co. Ltd., Beijing, China) and transferred to a computer through a USB interface for storage, processing, and display.

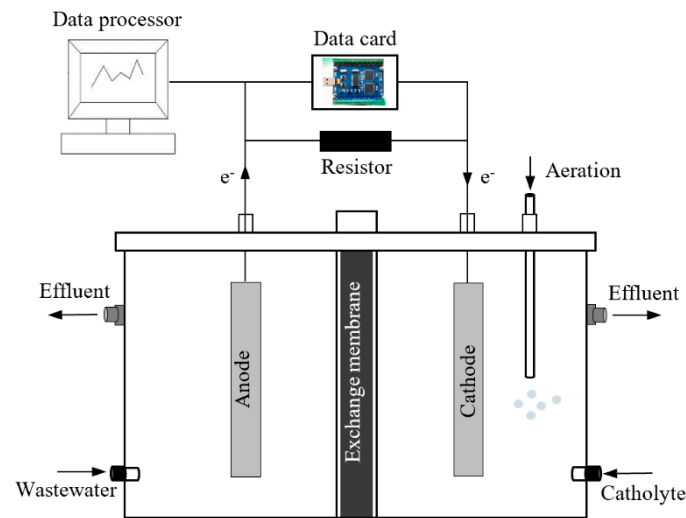


**Figure 1.** Schematic diagram of MFC experimental system.

## 2.2. Experimental Materials and Pretreatment

Molasses wastewater was used as the analyte of MFC in the experiment [41]. The molasses wastewater was made from the following chemicals: 3 g/L brown sugar, 3.13 g/L  $\text{NaHCO}_3$ , 0.31 g/L  $\text{NH}_4\text{Cl}$ , 6.338 g/L  $\text{NaH}_2\text{PO}_4 \cdot \text{H}_2\text{O}$ , 0.13 g/L  $\text{KCl}$ , 0.2 g/L  $\text{MgSO}_4 \cdot 7\text{H}_2\text{O}$ , 0.015 g/L  $\text{CaCl}_2$ , 0.01 g/L  $\text{MnSO}_4 \cdot \text{H}_2\text{O}$ , and 6.8556 g/L  $\text{Na}_2\text{HPO}_4 \cdot 12\text{H}_2\text{O}$ . All reagents used in the experiment were purchased from Tianjin Damao Company, Tianjin, China.

The catholyte was prepared by mixing potassium ferricyanide ( $\text{K}_3[\text{Fe}(\text{CN})_6]$ ) and sodium chloride ( $\text{NaCl}$ ) at a ratio of 1:1 [42]. First, 32.9 g  $\text{K}_3[\text{Fe}(\text{CN})_6]$  was dissolved with a concentration of 0.2 mol/L in phosphate buffer solution (PBS) in a 500 mL volumetric flask; then 11.7 g  $\text{NaCl}$  with the concentration of 0.4 mol/L was put into the other 500 mL volumetric flask; finally, the above-mentioned  $\text{K}_3[\text{Fe}(\text{CN})_6]$  solution and  $\text{NaCl}$  solution were mixed and the prepared catholyte was obtained.

Studies have shown that the soil contains a large number of microorganisms [43]. Therefore, soil under tree roots on the campus was collected and domesticated to obtain the required electricity-producing bacteria. The acclimation process was as follows: under anaerobic conditions, the prepared molasses wastewater and the collected soil were put into a culture bottle, some microelements such as carbon, nitrogen, and phosphorus required for the growth of microorganisms were added to it, and then the culture flask was put into a biochemical incubator and acclimated at 30 °C for three days. When the sludge in the culture bottle was suspended as a flocculate, it was considered that the sludge domestication was successful and could be used as a microbial species.

## 2.3. Preparation of Anode

First, the carbon felt was pretreated. The carbon felt was soaked in acetone for 2 h, then the soaked carbon felt was rinsed repeatedly with deionized water until neutral, then it was placed in a constant temperature drying oven at 65–85 °C to dry for standby.

Then, the pyrrole was polymerized on several pieces of carbon felt separately by potentiostatic deposition. A total of 0.05 mol pyrrole was dissolved in 500 mL distilled water as the electrolyte, and anodic electropolymerization was performed at a constant potential of 0.8 V with carbon felt as the working electrode, a platinum electrode as the counter electrode, and a saturated calomel electrode (SCE) as the reference electrode.  $\text{PPy}_{10}/\text{CF}$ ,  $\text{PPy}_{30}/\text{CF}$ ,  $\text{PPy}_{50}/\text{CF}$ , and  $\text{PPy}_{70}/\text{CF}$  composite anodes were prepared under the conditions of 10 min, 30 min, 50 min, and 70 min. The composite anodes were rinsed with deionized water, then air-dried at room temperature and stored for later use.

Finally, on the basis of the above treatment,  $\text{Fe}_3\text{O}_4$  particles were electrodeposited on  $\text{PPy}_{10}/\text{CF}$ ,  $\text{PPy}_{30}/\text{CF}$ ,  $\text{PPy}_{50}/\text{CF}$ , and  $\text{PPy}_{70}/\text{CF}$  composite anodes by cyclic voltammetry. A total of 0.96 g  $\text{Fe}_3\text{O}_4$  powder was added to the electrolyte of 500 mL PBS solution

with a concentration of 0.05 mol/L. The above four anodes were used as the working electrode separately, the platinum electrode and the saturated calomel electrode were used as the counter electrode and the reference electrode, respectively. Under the conditions of a scanning rate of 20 mV/s and potential range of  $-0.7$  V to  $0.7$  V, the pre-deposition was carried out for 10 min. Then  $\text{Fe}_3\text{O}_4\text{-PPy}_{10}/\text{CF}$ ,  $\text{Fe}_3\text{O}_4\text{-PPy}_{30}/\text{CF}$ ,  $\text{Fe}_3\text{O}_4\text{-PPy}_{50}/\text{CF}$ , and  $\text{Fe}_3\text{O}_4\text{-PPy}_{70}/\text{CF}$  composite anodes were obtained by electrodeposition for 20 min at  $-1.4$  V constant potential. The modified anodes were then rinsed with deionized water, dried in vacuum at  $60$  °C, and then stored for later use.

#### 2.4. Analytical Method

The current density  $I_A$  of the MFC was used to represent the power generation capacity. On the basis of the measured voltage, the effective anode surface area, and the value of the load resistance, the current density can be obtained through the following formula:

$$I_A = \frac{U}{RA} \quad (1)$$

where  $U$  is the output voltage of MFC measured by the data acquisition card;  $R$  is the load resistance; and  $A$  is the anode surface area. In the experiment, the load resistance was set to  $1000 \Omega$ .

In order to observe the surface characterization of the anodes in more depth, a scanning electron microscope (SEM) was used to characterize and analyze the carbon felt before and after modification. In addition, the cyclic voltammetry (CV) characteristics of the modified carbon felt were measured at room temperature using the three electrode system of the electrochemical workstation (CHI660E, CH Instrument Co., Shanghai, China), with the potential range of  $-0.6$  V to  $1.2$  V, and a scanning speed of  $5$  mV/s. Additionally, electrochemical impedance spectroscopy (EIS) analysis of the MFC was carried out.

The sewage disposal effect is also an important indicator to characterize the performance of MFC. The chemical oxygen demand (COD) value of the inlet and outlet of the anode chamber was measured by a COD rapid detector (LH-NP2, Dalian Luohand Biotech Co. Ltd., China), and then the COD removal rate  $COD_{rr}$  can be calculated by:

$$COD_{rr} = \frac{COD_{in} - COD_{out}}{COD_{in}} \times 100\% \quad (2)$$

where  $COD_{in}$  and  $COD_{out}$  represent the influent and effluent COD, respectively.

### 3. Results and Discussion

#### 3.1. Power Generation Performance

To obtain a good contrast effect, five groups of MFC experimental systems with the same structure and configuration were operated at the same time to ensure that other conditions except comparison items were the same.

The current density curves of MFC with the five different anodes are shown in Figure 2, where the horizontal axis time denotes the testing time of MFC, while the subscript number of "PPy" in the text description in the figure represents the electrodeposition time during electrode modification. The maximum output current density values of MFC with the  $\text{Fe}_3\text{O}_4\text{-PPy}_{10}$ ,  $\text{Fe}_3\text{O}_4\text{-PPy}_{30}$ ,  $\text{Fe}_3\text{O}_4\text{-PPy}_{50}$ , and  $\text{Fe}_3\text{O}_4\text{-PPy}_{70}$  modified carbon felt anodes were  $0.161 \text{ A/m}^2$ ,  $0.162 \text{ A/m}^2$ ,  $0.170 \text{ A/m}^2$ , and  $0.161 \text{ A/m}^2$ , respectively. The times required for the system to basically stabilize were about 86 h, 110 h, 80 h, and 115 h, respectively, and the corresponding steady-state current densities were  $0.151 \text{ A/m}^2$ ,  $0.157 \text{ A/m}^2$ ,  $0.166 \text{ A/m}^2$ , and  $0.151 \text{ A/m}^2$ , respectively. It can also be seen from Figure 2 that the maximum current density, steady value, and the stabilization time of MFC with the general carbon felt anode were  $0.104 \text{ A/m}^2$ ,  $0.099 \text{ A/m}^2$ , and 125 h, respectively. The experimental results suggest that the current density of MFC with the  $\text{Fe}_3\text{O}_4\text{-PPy}$  composite modified carbon felt anode was significantly improved, indicating that  $\text{Fe}_3\text{O}_4\text{-PPy}$  composite had a better effect as an anode modified material of MFC. The current densities of MFC with

$\text{Fe}_3\text{O}_4\text{-PPy}_{10}$ ,  $\text{Fe}_3\text{O}_4\text{-PPy}_{30}$ ,  $\text{Fe}_3\text{O}_4\text{-PPy}_{50}$ , and  $\text{Fe}_3\text{O}_4\text{-PPy}_{70}$  modified carbon felt anodes increased by 50.1%, 52.5%, 59.5%, and 54.6%, respectively, compared with that of MFC with the unmodified anode. Among them, when the PPy deposition time was increased from 10 min to 30 min and 50 min, the output current density of MFC increased sequentially, and the output current density reached the maximum when the PPy deposition time extended to 50 min. However, when the deposition time continued to extend to 70 min, the output current density no longer increased but decreased. This indicates that the effect of anode modification is not proportional to the deposition time. Excessive deposition of PPy on the carbon felt will inhibit the power generation performance of MFC. Under the experimental conditions in this paper, the most appropriate electrodeposition time was 50 min.

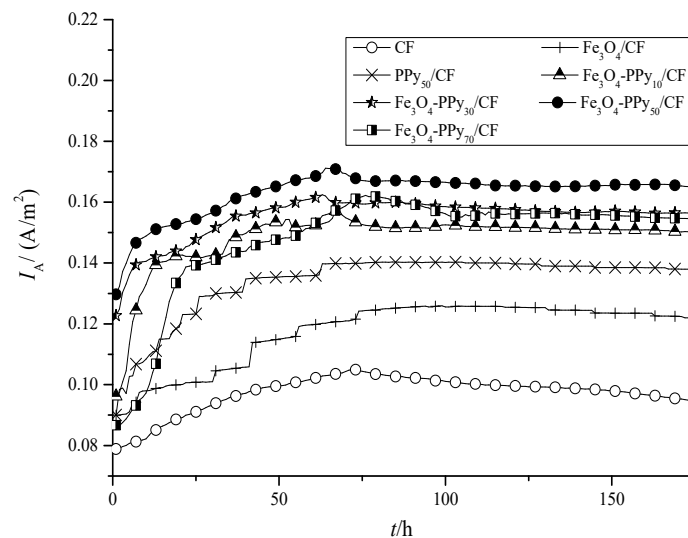


**Figure 2.** The output current density of MFC with different anodes.

On the other hand, it was observed that the current density of CF decreased obviously with time in the long run, whereas that for the modified composite anode did not. This may be because the carbon felt that has run for a long time absorbs too much sludge and other non-conductive impurities, which leads to the pore blockage and the reduction of the specific surface area, thus leading to the reduction in electricity generation performance. However, for the modified anode, the surface is rich in conductive particles, so it is not easy to absorb sludge, and the conductive composite material attached to the surface also increases the specific surface area of the anode, thus improving the stability of conductivity.

In order to distinguish the synergistic effect of PPy and  $\text{Fe}_3\text{O}_4$ , the current density of MFC with PPy and  $\text{Fe}_3\text{O}_4$  modified anode was also measured and is shown in Figure 2. It can be seen that the current density of MFC with the PPy or  $\text{Fe}_3\text{O}_4$  modified anode was much smaller than that of MFC with the  $\text{Fe}_3\text{O}_4\text{-PPy}$  composite modified anode. This indicates that the  $\text{Fe}_3\text{O}_4\text{-PPy}$  composite material significantly improved the electrode modification effect.

### 3.2. SEM Analysis

The SEM images of the  $\text{Fe}_3\text{O}_4\text{-PPy}_{10}$ ,  $\text{Fe}_3\text{O}_4\text{-PPy}_{30}$ ,  $\text{Fe}_3\text{O}_4\text{-PPy}_{50}$ , and  $\text{Fe}_3\text{O}_4\text{-PPy}_{70}$  modified carbon felt anodes are given in Figure 3. It can be seen that, within 50 min, with the increase in electrodeposition time, the content of particles deposited on the electrode surface increased gradually; especially when the deposition time reached 50 min, a large number of conductive particles was deposited on the electrode surface, which enlarged the specific surface area of the electrode significantly. However, when the deposition time reached 70 min, there was no obvious particle deposition on the electrode surface, and the specific surface had no obvious improvement compared with the unmodified electrode.



This further proves that the electrodeposition time of 50 min is the most suitable for anode modification using the  $\text{Fe}_3\text{O}_4$ -PPy composite material, while a longer electrodeposition time is not conducive to the deposition of conductive particles on the electrode surface.

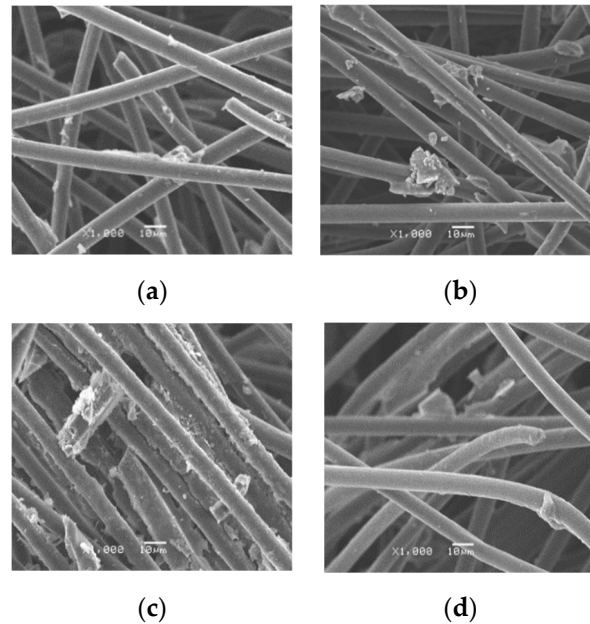


**Figure 3.** SEM image of the modified anodes. (a)  $\text{Fe}_3\text{O}_4$ -PPy<sub>10</sub>/CF; (b)  $\text{Fe}_3\text{O}_4$ -PPy<sub>30</sub>/CF; (c)  $\text{Fe}_3\text{O}_4$ -PPy<sub>50</sub>/CF; (d)  $\text{Fe}_3\text{O}_4$ -PPy<sub>70</sub>/CF.

### 3.3. CV Characteristics

The cyclic voltammetry (CV) curves of the four different anodes are shown in Figure 4. It can be seen that the anodes modified with  $\text{Fe}_3\text{O}_4$ -PPy had obvious oxidation peaks and reduction peaks. This is because  $\text{Fe}_3\text{O}_4$  and PPy change the specific surface area and roughness of the anode, which provides better conditions for microorganisms to attach in, and thus the peak value of redox current increases accordingly. This indicates that  $\text{Fe}_3\text{O}_4$ -PPy modified anodes can significantly improve the activity of electrochemical reaction. In particular, when the electrochemical deposition time was 50 min, the modified anode provided the highest redox current, which indicates that the  $\text{Fe}_3\text{O}_4$ -PPy<sub>50</sub>/CF anode had greater redox activity and a larger electrochemically active surface area, and the anode modification effect was the best in this case.

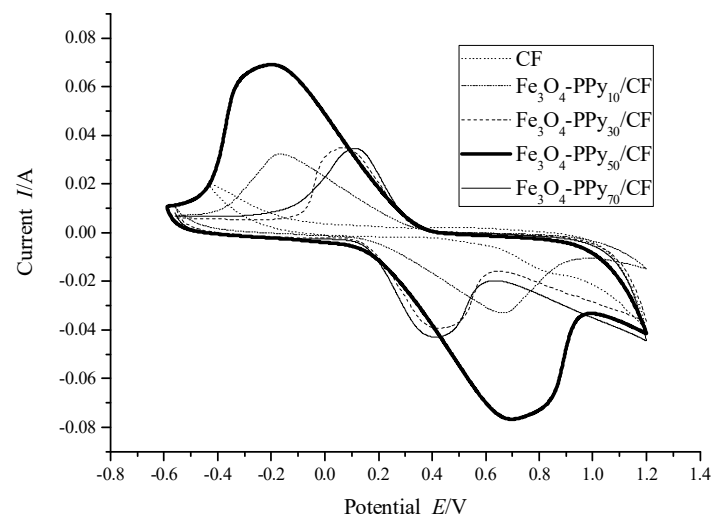


**Figure 4.** CV curves of the four different anodes.

### 3.4. EIS Analysis

The internal resistance is also an important factor affecting the MFC's performance. Electrochemical impedance spectroscopy (EIS) can reflect the impedance information of the whole MFC system. The electrochemical impedance spectra of MFC with different modified anodes are shown in Figure 5. The value of the left intersection of the semicircle and the horizontal axis denotes the solution internal resistance; the diameter of the semicircle denotes the charge transfer resistance caused by the oxidation-reduction reaction on the electrode surface; and the inclined straight line in the high frequency region represents the diffusion impedance [44].

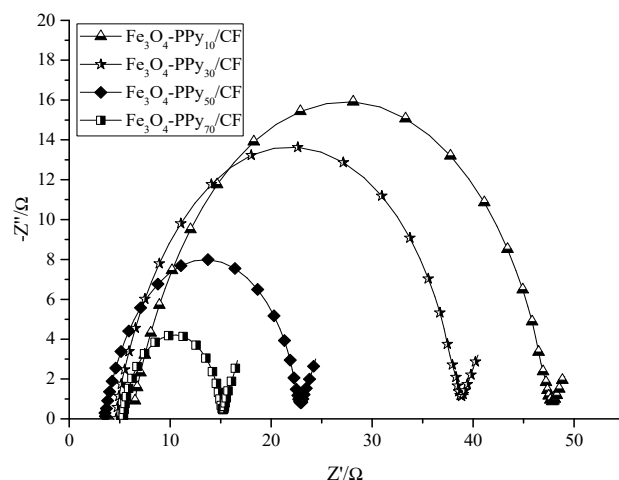


**Figure 5.** Electrochemical impedance spectra of MFC with different modified anodes.

The EIS spectra showed that the solution's internal resistances of MFC with  $\text{Fe}_3\text{O}_4\text{-PPy}_{10}$ ,  $\text{Fe}_3\text{O}_4\text{-PPy}_{30}$ , and  $\text{Fe}_3\text{O}_4\text{-PPy}_{50}$  modified anodes were about  $6.518 \Omega$ ,  $4.658 \Omega$ , and  $3.539 \Omega$ , respectively, and the corresponding charge transfer impedances were  $41.58 \Omega$ ,  $34.53 \Omega$ , and  $19.73 \Omega$ , respectively. It can be seen that when the electrodeposition time was 50 min, the solution internal resistance and charge transfer resistance of MFC were less than those when the anode electrodeposition time was 10 min and 30 min, indicating that the resistance of the MFC reactor decreased with the appropriate increase in pyrrole polymerization time.

The EIS spectra also showed that the solution internal resistance of MFC with the  $\text{Fe}_3\text{O}_4\text{-PPy}_{70}$  modified anode was  $5.35 \Omega$ , which means that when the electrodeposition time exceeded 50 min, the solution resistance of MFC increased rather than decreased with the further increase in the electrodeposition time. In a word, when the electrodeposition time was 50 min, the solution internal resistance of MFC was the minimum, so 50 min was the most suitable electrodeposition time for the preparation of the  $\text{Fe}_3\text{O}_4\text{-PPy}$  modified anode. The equivalent circuit is shown in Figure 6, where  $R_s$  denotes the solution internal resistance of MFC;  $R_{CT}$  is the charge transfer impedance;  $Z_W$  is the Warburg impedance that reflects the resistance encountered by the reactants in the process of diffusion in solution, and CPE is a constant phase element represented by a double-layer impedance.

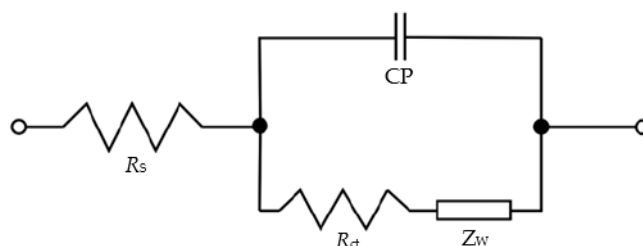


**Figure 6.** The equivalent circuit of MFC.

### 3.5. Water Quality Analysis

Sewage treatment efficiency is also a crucial indicator reflecting the performance of MFC. In this experiment, molasses wastewater was the main raw material for MFC power generation, and the COD removal rate was used to evaluate the sewage treatment efficiency of MFCs. Table 1 shows the COD values of the inlet and outlet water of MFCs with different modified anodes. It can be seen that the COD removal rates of MFC with the unmodified carbon felt anode and the Fe<sub>3</sub>O<sub>4</sub>-PPy<sub>10</sub>/CF, Fe<sub>3</sub>O<sub>4</sub>-PPy<sub>30</sub>/CF, Fe<sub>3</sub>O<sub>4</sub>-PPy<sub>50</sub>/CF, and Fe<sub>3</sub>O<sub>4</sub>-PPy<sub>70</sub>/CF anodes were 27.8%, 42.8%, 48.8%, 55.1%, and 46.5%, respectively. The water purification effect of MFC with the Fe<sub>3</sub>O<sub>4</sub>-PPy modified anode was significantly improved. It can be seen from the results that, in a certain period of time, the water purification effect increased with the increase in electrodeposition time, and reached the best when the deposition time was 50 min. The COD removal rate of MFC with Fe<sub>3</sub>O<sub>4</sub>-PPy<sub>50</sub>/CF anode was 95.3% higher than that of MFC with the unmodified anode. However, with the further increase in electrodeposition time, the water purification effect showed a downward trend. This further proves that the electrode modification effect is not completely proportional to the electrodeposition time. The electrodeposition time is an important factor affecting the performance of the electrode. Proper electrodeposition time is the key to improving the conductive property of the anode and enhancing the power production capacity and sewage treatment efficiency of MFC.

**Table 1.** COD removal rate of MFC under different deposition time modified anode.

	Blank	Fe <sub>3</sub> O <sub>4</sub> -PPy <sub>10</sub> /CF	Fe <sub>3</sub> O <sub>4</sub> -PPy <sub>30</sub> /CF	Fe <sub>3</sub> O <sub>4</sub> -PPy <sub>50</sub> /CF	Fe <sub>3</sub> O <sub>4</sub> -PPy <sub>70</sub> /CF
COD <sub>in</sub> (mg/L)	7545	7545	7545	7545	7545
COD <sub>out</sub> (mg/L)	5445	4315	3895	3390	4035
COD <sub>rr</sub> (%)	27.8%	42.8%	48.4%	55.1%	46.5%

Molasses wastewater belongs to high-concentration organic wastewater with high COD content. The COD removal rate of molasses wastewater treated by MFC with the Fe<sub>3</sub>O<sub>4</sub>-PPy composite modified anode could reach more than 55%, indicating that MFC is useful for degrading molasses wastewater and generating electricity at the same time.

### 4. Conclusions

Fe<sub>3</sub>O<sub>4</sub> has strong conductivity and the conductive polymer PPy has excellent biocompatibility. By depositing Fe<sub>3</sub>O<sub>4</sub> and PPy on the carbon felt anode, the synergistic effect of the two can significantly improve the power generation capacity of MFC. Therefore, Fe<sub>3</sub>O<sub>4</sub>-PPy composites are a very effective anode modification material that can significantly improve the electricity generation performance and water purification effect of MFC.

In addition, the electrodeposition time is an important factor affecting the effect of anode modification. The conductivity of the anode does not always increase with the increase in electrodeposition time, but there is a peak point. This study showed that when Fe<sub>3</sub>O<sub>4</sub>-PPy composites were used to modify the carbon felt electrode, the generation current density and COD removal rate of MFC were the best when the electrodeposition time was 50 min. In this case, the steady state current density was 0.166 A/m<sup>2</sup>, which was 59.5% higher than that of the unmodified anode; the COD removal rate was 55.1%, which was 95.3% higher than that of the unmodified anode; in particular, the MFC with the Fe<sub>3</sub>O<sub>4</sub>-PPy<sub>50</sub> modified anode could reach the steady state faster, and the time to reach the steady state was 36% less than that of the MFC with the common carbon felt anode. Therefore, when the electrodeposition time is suitable, modifying the anode with the Fe<sub>3</sub>O<sub>4</sub>-PPy composites is an available method to raise the MFC performance.

**Author Contributions:** Conceptualization, L.F.; Data curation, Y.X.; Formal analysis, Y.X.; Investigation, L.F. and Y.X.; Methodology, L.F.; Project administration, L.F.; Resources, L.F.; Validation, Y.X.; Visualization, L.F.; Writing—original draft, Y.X.; Writing—review & editing, L.F. All authors have read and agreed to the published version of the manuscript.



**Funding:** This work was funded by the National Natural Science Foundation of China (grant 61143007); the Chinese-Macedonian Scientific and Technological Cooperation Project of Ministry of Science and Technology of the People's Republic of China (grant [2019] 22:6-8), and the Plan for Distinguished Professors in Liaoning Province, China (grant [2014] 187).

**Conflicts of Interest:** The authors declare no conflict of interest.

## References

1. Ray, P. Renewable energy and sustainability. *Clean Technol. Environ.* **2019**, *21*, 1517–1533. [[CrossRef](#)]
2. Salihu, M.D.; Zhonghua, T.; Ibrahim, A.O.; Habib, M. China's energy status: A critical look at fossils and renewable options. *Renew. Sustain. Energy Rev.* **2017**, *81*, 2281–2290.
3. Feng, T.T.; Yang, Y.S.; Xie, S.Y.; Dong, J.; Ding, L. Economic drivers of greenhouse gas emissions in China. *Renew. Sustain. Energy Rev.* **2017**, *78*, 996–1006. [[CrossRef](#)]
4. Pratiwi, S.; Juerges, N. Review of the impact of renewable energy development on the environment and nature conservation in Southeast Asia. *Energy Ecol. Environ.* **2020**, *5*, 221–239. [[CrossRef](#)]
5. Kose, N.; Bekun, F.V.; Alola, A.A. Criticality of sustainable Research and Development-led Growth in EU: The role of Renewable and Non-Renewable Energy. *Environ. Sci. Pollut. Res.* **2020**, *27*, 12683–12691. [[CrossRef](#)]
6. Usman, O.; Akadiri, S.S.; Adeshola, I. Role of renewable energy and globalization on ecological footprint in the USA: Implications for environmental sustainability. *Environ. Sci. Pollut. Res.* **2020**, *27*, 30681–30693. [[CrossRef](#)]
7. Palanisamy, G.; Jung, H.Y.; Sadhasivam, T.; Kurkuri, M.D.; Kim, S.C.; Roh, S.H. A comprehensive review on microbial fuel cell technologies: Processes, utilization, and advanced developments in electrodes and membranes. *J. Clean. Prod.* **2019**, *221*, 598–621. [[CrossRef](#)]
8. Munoz-Cupa, C.; Hu, Y.; Xu, C.; Bassi, A. An overview of microbial fuel cell usage in wastewater treatment, resource recovery and energy production. *Sci. Total Environ.* **2021**, *754*, 142429. [[CrossRef](#)] [[PubMed](#)]
9. Nishat, K.; Danish, K.M.; Abdul-Sattar, N.; Mohammad, R.; Azfar, S.; Anees, A.; Khan, M.Z. Energy generation through bioelectrochemical degradation of pentachlorophenol in microbial fuel cell. *RSC Adv.* **2018**, *8*, 20726–20736.
10. Jatoi, A.S.; Akhter, F.; Mazari, S.A.; Sabzoi, N.; Ahmed, S. Advanced microbial fuel cell for waste water treatment—a review. *Environ. Sci. Pollut. Res.* **2021**, *28*, 5005–5019. [[CrossRef](#)]
11. Kumar, S.S.; Kumar, V.; Kumar, R.; Malyan, S.K.; Pugazhendhi, A. Microbial fuel cells as a sustainable platform technology for bioenergy, biosensing, environmental monitoring, and other low power device applications. *Fuel* **2019**, *255*, 115682. [[CrossRef](#)]
12. Fan, L.P.; Shi, J.Y.; Gao, T. Comparative Study on the Effects of Three Membrane Modification Methods on the Performance of Microbial Fuel Cell. *Energies* **2020**, *13*, 1383. [[CrossRef](#)]
13. Zhao, F.; Rahunen, N.; Varcoe, J.R.; Roberts, A.J.; Avignone-Rossa, C.; Thumser, A.E.; Slade, R.C.T. Factors affecting the performance of microbial fuel cells for sulfur pollutants removal. *Biosens. Bioelectron.* **2009**, *24*, 1931–1936. [[CrossRef](#)]
14. Fan, L.P.; Miao, X.H. Study on the performance of microbial fuel cell for restaurant wastewater treatment and simultaneous electricity generation. *J. Fuel Chem. Technol.* **2014**, *42*, 1506–1512.
15. You, J.; Santoro, C.; Greenman, J.; Melhuish, C.; Cristiani, P.; Li, B.; Ieropoulos, I. Micro-porous layer (MPL)-based anode for microbial fuel cells. *Int. J. Hydrogen Energy* **2014**, *39*, 21811–21818. [[CrossRef](#)]
16. Fan, L.P.; Bao, W.F. Effects of K<sub>2</sub>Cr<sub>2</sub>O<sub>7</sub> and KClO<sub>3</sub> modified anode on MFC performance. *J. Chem. Eng. Chin. Univ.* **2019**, *33*, 758–764.
17. Sreelekshmy, B.R.; Rajappan, A.J.; Basheer, R.; Vasudevan, V.; Shibli, S.M.A. Tuning of Surface Characteristics of Anodes for Efficient and Sustained Power Generation in Microbial Fuel Cells. *ACS Appl. Biol. Mater.* **2020**, *3*, 6224–6236. [[CrossRef](#)]
18. Hamed, M.S.; Majdi, H.S.; Hasan, B.O. Effect of Electrode Material and Hydrodynamics on the Produced Current in Double Chamber Microbial Fuel Cells. *ACS Omega* **2020**, *5*, 10339–10348. [[CrossRef](#)] [[PubMed](#)]
19. Zhu, X.; Logan, B.E. Copper anode corrosion affects power generation in microbial fuel cells. *J. Chem. Technol. Biot.* **2014**, *89*, 471–474. [[CrossRef](#)]
20. Cai, T.; Meng, L.J.; Chen, G.; Xi, Y.; Jiang, N.; Song, J.L.; Zheng, S.Y.; Liu, Y.B.; Zhen, G.Y.; Huang, M.H. Application of advanced anodes in microbial fuel cells for power generation: A review. *Chemosphere* **2020**, *248*, 125985. [[CrossRef](#)]
21. Yaqoob, A.A.; Ibrahim, M.N.M.; Rafatullah, M.; Yong, S.C.; Ahmad, A.; Umar, K. Recent Advances in Anodes for Microbial Fuel Cells: An Overview. *Materials* **2020**, *13*, 2078. [[CrossRef](#)]
22. Li, B.; Zhao, Z.; Weng, Z.; Fang, Y.; Lei, W.; Zhu, D.; Jiang, H.; Mohtar, M.N.B.; Halin, I.B.A. Modification of PPy-NW Anode by Carbon Dots for High-performance Mini-microbial Fuel Cells. *Fuel Cells* **2020**, *20*, 203–211. [[CrossRef](#)]
23. Fan, M.; Chen, X.; Zhou, Y.; Chen, Y.; Shen, S. Improved Bioactivity on Substrate Degradation in Microbial Fuel Cells Using Tourmaline-Modified Anodes. *J. Environ. Eng.* **2019**, *145*, 06019003. [[CrossRef](#)]
24. Iftimie, S.; Dumitru, A. Enhancing the performance of microbial fuel cells (MFCs) with nitrophenyl modified carbon nanotubes-based anodes. *Appl. Surf. Sci.* **2019**, *492*, 661–668. [[CrossRef](#)]
25. Nosek, D.; Jachimowicz, P.; Cydzik-Kwiatkowska, A. Anode Modification as an Alternative Approach to Improve Electricity Generation in Microbial Fuel Cells. *Energies* **2020**, *13*, 6596. [[CrossRef](#)]
26. Yin, Y.; Huang, G.; Zhou, N.; Liu, Y.; Zhang, L. Increasing power generation of microbial fuel cells with a nano-CeO<sub>2</sub> modified anode. *Energy Sources Part A* **2016**, *38*, 1212–1218. [[CrossRef](#)]

27. Senthilkumar, N.; Pannippara, M.; Al-Sehemi, A.G.; George, G.K. PEDOT/NiFe<sub>2</sub>O<sub>4</sub> nanocomposite on biochar as a free standing anode for high performance and durable microbial fuel cells. *New J. Chem.* **2019**, *43*, 7743–7750. [[CrossRef](#)]
28. Zhang, H.; Fu, Y.; Zhou, C.; Liu, S.; Zhao, M.; Chen, T.; Zai, X. A novel anode modified by 1,5-dihydroxyanthraquinone/multiwalled carbon nanotubes composite in marine sediment microbial fuel cell and its electrochemical performance. *Int. J. Energy Res.* **2018**, *42*, 2574–2582. [[CrossRef](#)]
29. Wu, X.; Xiong, X.; Brunetti, G.; Yong, X.; Zhou, J.; Zhang, L.; Wei, P.; Jia, H. Effect of MWCNT-modified graphite felts on hexavalent chromium removal in biocathode microbial fuel cells. *RSC Adv.* **2017**, *7*, 53932–53940. [[CrossRef](#)]
30. Sonawane, J.M.; Ghosh, P.C.; Samuel, A. Electrokinetic behaviour of conducting polymer modified stainless steel anodes during the enrichment phase in microbial fuel cells. *Electrochim. Acta* **2018**, *287*, 95–105. [[CrossRef](#)]
31. Ouis, M.; Kameche, M.; Innocent, C.; Charef, M.; Kebaili, H. Electro-polymerization of pyrrole on graphite electrode: Enhancement of electron transfer in bioanode of microbial fuel cell. *Polym. Bull.* **2018**, *75*, 669–684. [[CrossRef](#)]
32. Kisieliute, A.; Popov, A.; Apetrei, R.M.; Carac, G.; Morkvenaite-Vilkonciene, I.; Ramanaviciene, A.; Ramanavicius, A. Towards microbial biofuel cells: Improvement of charge transfer by self-modification of microorganisms with conducting polymer-Polypyrrole. *Chem. Eng. J.* **2019**, *356*, 1014–1021. [[CrossRef](#)]
33. Pareek, A.; Shanthi Sravan, J.; Venkata Mohan, S. Graphene modified electrodes for bioelectricity generation in mediator-less microbial fuel cell. *J. Mater. Sci.* **2019**, *54*, 11604–11617. [[CrossRef](#)]
34. Yuan, H.; He, Z. Graphene-modified electrodes for enhancing the performance of microbial fuel cells. *Nanoscale* **2015**, *7*, 7022–7029. [[CrossRef](#)]
35. Hindatu, Y.; Annuar, M.S.M.; Gumel, A.M. Mini-review: Anode modification for improved performance of microbial fuel cell. *Renew. Sustain. Energy Rev.* **2017**, *73*, 236–248. [[CrossRef](#)]
36. Yu, B.; Li, Y.; Feng, L. Enhancing the performance of soil microbial fuel cells by using a bentonite-Fe and Fe<sub>3</sub>O<sub>4</sub> modified anode. *J. Hazard Mater.* **2019**, *377*, 70–77. [[CrossRef](#)]
37. Xing, L.; Wu, W.; Gu, Z. Poly (3,4-ethylenedioxythiophene) promotes direct electron transfer at the interface between *Shewanella loihica* and the anode in a microbial fuel cell. *J. Power Sources* **2015**, *277*, 110–115.
38. Qi, Y.; Nguyen, M.H.T.; Oh, E.S. Enhancement of the lithium titanium oxide anode performance by the copolymerization of conductive polypyrrole with poly(acrylonitrile/butyl acrylate) binder. *J. Appl. Electrochem.* **2020**, *50*, 431–438. [[CrossRef](#)]
39. Lv, Y.; Shang, M.; Chen, X.; Nezhad, P.; Niu, J. Largely Improved Battery Performance Using a Microsized Silicon Skeleton Caged by Polypyrrole as Anode. *ACS Nano* **2019**, *13*, 12032–12041. [[CrossRef](#)]
40. Pu, K.B.; Lu, C.X.; Zhang, K.; Zhang, H.; Chen, Q.Y.; Wang, Y.H. In situ synthesis of polypyrrole on graphite felt as bio-anode to enhance the start-up performance of microbial fuel cells. *Bioproc. Biosyst. Eng.* **2020**, *43*, 429–437. [[CrossRef](#)]
41. Fan, L.P.; Xu, D.D.; Li, C.; Xue, S. Molasses wastewater treatment by microbial fuel cell with MnO<sub>2</sub> modified cathode. *Pol. J. Environ. Stud.* **2016**, *25*, 2359–2356. [[CrossRef](#)]
42. Fan, L.P.; Zheng, Y.J.; Miao, X.H. Effects of catholyte and dissolved oxygen on microbial fuel cell performance. *J. Chem. Eng. Chin. Univ.* **2016**, *30*, 491–496.
43. Islam, M.A.; Ethiraj, B.; Cheng, C.K.; Yousuf, A.; Khan, M.M.R. Electrogenic and antimethanogenic properties of *Bacillus cereus* for enhanced power generation in anaerobic sludge-driven microbial fuel cells. *Energy Fuel* **2017**, *31*, 6132–6139. [[CrossRef](#)]
44. Fan, L.P.; Shi, J.Y.; Xi, Y.B. PVDF-modified Nafion membrane for improved performance of MFC. *Membranes* **2020**, *10*, 185. [[CrossRef](#)] [[PubMed](#)]